*Accepted for publication by Proc IMechE Part C: J Mechanical Engineering Science, 16 September 2016, DOI: 10.1177/0954406216673396*

# Energy transfer in a beam-framed structure using a modal method and a wave method at mid-frequencies

J. W. Yoo[1], D. J. Thompson[2] and N. S. Ferguson[2]

## Abstract

A fully framed system consisting of four beams and a rectangular plate has been investigated in terms of the energy transfer between the beams and the plate when a force is applied to one of the beams. This configuration, which is a mixture of stiff and flexible elements, is a particularly important example in the industrial area, as it is widely used. A modal model based on interface basis functions is used. A wave model, which is an approximate method, has also been developed in which the plate, acting as a wave impedance, is separately attached to each beam. Experimental studies have been carried out for validation. The investigation with respect to power flow and energy shows the validity of both models in the mid-frequency region. The results show that most energy is dissipated by the flexible plate. The physical phenomena and limitations of the wave method for this particular structural configuration are discussed. Even though it is an approximate method, the wave approach can describe the dynamic characteristics of the excited beam and the plate in terms of the ratios of power and energy of each component. The comparison of the two methods shows that the plate rather than the beams plays a crucial role in transferring the energy from the excited beam to the parallel opposite beam in the beam-framed structure when these two beams have identical properties, whereas the energy transfer is reduced when the beams have dissimilar properties.

**Keywords:** framed structure, beam, plate, wave method, modal method, mid-frequency, energy ratio, power

## 1. Introduction

Beam-plate coupled structures are widely used in many industrial fields; these generally consist of stiff beams connected to more flexible plates. An automotive vehicle, for example, has a floor made of stiff beams with flexible plates between them. The stiff beams are often excited by the external loads, and vibration energy is transmitted to the

[1] Noise and Vibration CAE Team, Hyundai-Kia Motors, Korea
[2] Institute of Sound and Vibration Research, University of Southampton, Southampton, SO17 1BJ, United Kingdom

**Corresponding author:**
Noise and Vibration CAE Team, Research and Development Division, Hyundai-Kia Motors, 150, Hyundaiyeonguso-ro, Hwaseong-si, 18280, Korea
Email: j.w.yoo@hyundai.com

plates. The plates radiate most of the noise. Therefore, there have been many studies dealing with the noise and vibration of these types of structures.

The simplest such structure is a single beam coupled to a single plate. Grice and Pinnington [1] studied a single beam coupled to a single rectangular plate, introducing a wave approach. The excited stiff beam, referred to as the structural spine, transfers the energy to the flexible plate, which acts as a receiver. The study showed that the plate acts like damping to the beam.

The authors have used a wave-based approach [2,3] to investigate a coupled system consisting of two stiff beams and a flexible plate. By using symmetrical and anti-symmetrical conditions, it was shown that approximate dynamic behaviours of a beam-plate-beam system can be predicted.

Rumerman [4] introduced a model of a ribbed plate. The response of a uniform infinite plate, stiffened by a set of uniform ribs was studied by a Fourier transform approach. If the ribs are periodically located for a point excitation, the model can be expressed in a simple form in terms of line impedances and wavenumbers. The phyiscal concept of the line impedance is similar to that used in the present paper.

Legault and Atalla [5] used a wave-based model to investigate sound transmission through double panel structures with periodically spaced resilient mounts. A four pole formulation was employed for modelling the mount. The influence of mount spacing, cavity absorption and panel damping is studied. This periodic wave model was compared to a finite element and boundary element (FEM-BEM) model for structure-borne transmission. The wave model gave good approximation at mid- and high frequencies, although motion could not be captured precisely at low frequencies.

Hammer and Petersson [6] used a mobility technique to understand dynamic behaviours of a strip coupled to an infinite flexible plate. The study showed that the directivity of the farfield intensity from the source into the vibration field of the plate is uniform for small Helmholtz number. It becomes non-uniform for large number with its main lobe perpendicular to the strip.

Dickow et al [7] used a modal model to investigate a spatially periodic ribbed plate. A rectangular plate stiffened by several beams was assumed in the pinned conditions along all four edges. The modal model is similar with that given in the present paper, in that plate and beam modal matrices are combined; however in the current paper interface basis functions are introduced. According to the effects of the ribs, the modes could be divided into two groups: one showing periodic behaviour in terms of pass-bands and stop-bands, and another that shows less such behaviour.

In addition to these studies, various analytical methods [8,9] have been applied to a simple beam-plate coupled system; however, their applicability to more complex structures is yet to be determined.

Here, a straightforward and practical approach is sought for a complex industrial application. In this context, a framed system consisting of four stiff beams and a flexible

plate is considered as an example of a practical structure widely present in an automotive body structure, aircraft fuselage and ship hull [10].

Some published studies on frame-like structures exist. Takabatake and Nagareda [11] and Yang and Gupta [12] investigated the behaviour of a framed structure; however, both studies concentrated on predicting the plate behaviour rather than that of the beam. Also, in both papers, it was assumed that the motion of the ends of each beam is zero. Based on the point of view that the stiff beams possess long bending waves that transmit short-wavelength bending waves into the plate, the behaviour of the beams is very important [1].

Grice and Pinnington extended the wave method to form a hybrid method [13] in which a box structure was modelled. The finite element method was used to predict a long-wave response, and analytical impedances were considered to calculate short flexural waves.

An alternative hybrid method incorporating both the Finite Element Method (FEM) and Statistical Energy Analysis (SEA) was proposed by Langley et al. [14] in which separate direct and reverberant fields were introduced. A beam framework with three plates was investigated as an example.

Apart from this, there are few previous studies that investigated a frame-like system consisting of several beams coupled to a plate, and this configuration provides the motivation of the present research.

The frequency range of interest in this paper belongs to the mid-frequency region [15]. This can be defined as the frequency range in which some of the components of a system are suitable for treatment using a deterministic method, whilst other components are amenable to a statistical method. For coupled beam-plate structures, the mid-frequency region in this sense can be considered as the range in which the stiff beams show low frequency behaviour consisting of relatively few, well separated modes, while the flexible plates show high frequency behaviour consisting of many overlapping modes.

In this frequency region, particular modes and peaks are not of direct interest, but energy relationships, such as the power and energy ratio between subsystems, will be more important. For example, for a structure consisting of several beams, with excitation on one of the beams, and flexible plates which radiate noise, understanding the relationship of the energy transfer between beams and plates is most critical.

This paper, therefore, aims to consider the possibility for the analysis and understanding of the behaviour of more complicated structures in the mid-frequency region. In particular a four-beam coupled system is considered as this is relatively straightforward and intuitive for practical industrial application.

The numerical results from two methods are compared, a wave method and a modal method. The wave method is compact and uses few computer resources compared to the modal method. Whereas the wave method is approximate but practically suited for the

mid-frequency analysis, a modal model is considered as an exact solution for the given boundary conditions. A general coupling concept is introduced first to consider the coupling between the beams and plate.

As most vibration energy in the mid-frequency region is related to the flexural motion and in-plane motion mainly occurs at relatively higher frequencies, only transverse excitation and flexural motion are considered throughout this paper. Comparison with experiments shows such assumption is acceptable. Nevertheless the methods used could also be extended to include in-plane motion. For simplicity, the beams are modelled using the Euler-Bernoulli beam theory, and an isotropic rectangular plate is assumed [16]. It is assumed that the beams were infinitely stiff to torsion, and the plate is rigidly attached to the beams. Consequently, the edges of the plate and the beam ends are effectively sliding. This allows both an external excitation on an arbitrary location on the beam framework and a simplification for the modal method analysis. A wave model can be realised for the excited stiff beam which transfers the energy to the flexible plate.

Experimental validation is included in terms of the power and the energy ratio between the subsystems. By comparing the experimental results with the modal and the wave models, a better understanding of the energy transfer relationship between subsystems is expected.

The novelty of this work lies in the realisation of a framed structure of stiff beams and a flexible plate by both modal and wave methods. The plate-decoupled wave model shows reasonable power relationship at mid-frequencies (therefore, in terms of one-third octave band averages). The modal model, greatly simplified using sliding edge conditions, still gives more accurate result. Also, it is newly discovered that the energy transmission from the driven beam to the opposite beam changes dependent on the beam properties in this framed structure.

## 2. A modal formulation for the coupled motion of a system of two or four beams attached to a plate

### 2.1. General coupling based on a modal method

Although this paper emphasizes a coupled structure consisting of beams and a plate for sliding boundary conditions, the coupling in a general situation is presented first. The derivation is similar to Ji et al [17] but uses a dynamic stiffness approach [18] rather than a mobility approach.

Consider a coupled structure consisting of two subsystems attached through arbitrary continuous interfaces (see Figure 1). It is assumed initially for simplicity that the subsystems are undamped, although the damped system can also be realised simply by introducing a loss factor. For consistency with the following sections, the source subsystem is described as system '*b*' and the receiver subsystem as system '*p*', although at this stage the subsystems are not limited to beams and plates. An external force $f_e$ is applied to system *b* and the forces acting on each subsystem through the interface are given by $f_i^b$ and $f_i^p$ respectively. Although they will be enforced to be the same by an

equilibrium condition, they are initially described separately to explain the general coupling procedure.

The dynamic displacement of subsystem *b* can be written as [19]

$$w_b(\mathbf{x}_b) = \sum_m \phi_m^b(\mathbf{x}_b)\, q_m^b(t) \tag{1}$$

where $w_b(\mathbf{x}_b)$ is the displacement, $\phi_m^b$ is the *m*th mode shape function defining the shapes of the modes of vibration, $q_m^b$ is the *m*th generalised coordinate from which the subsystem motion is fully described by all of these coordinates and $\mathbf{x}_b$ is the local coordinate of subsystem *b* which is given in vector form. The displacement $w_b$ can be any direction at this stage, although only flexural motion will be considered for beam-plate coupled structures.

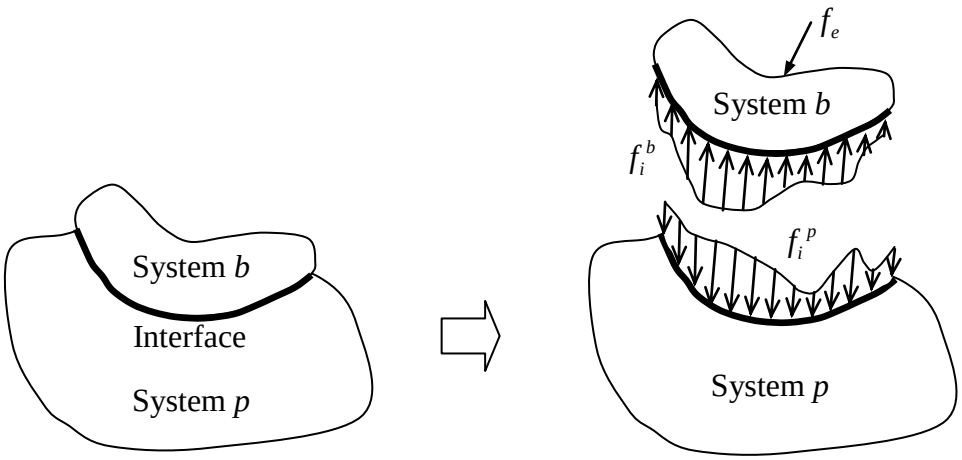


Figure 1. The coupled system and its force relationship between subsystems.

Assuming time-harmonic motion at angular frequency $\omega$, the steady state solution can be found as [17]

$$\mathbf{q}_b = \mathbf{S}_b^{-1}\left(\mathbf{F}_e^b - \mathbf{F}_i^b\right) \tag{2}$$

where $\mathbf{q}_b$ is the vector of generalised coordinate amplitudes, $\mathbf{S}_b$ is a diagonal matrix of modal stiffnesses, the elements of which are given by $S_m^b = M_m^b\left(\omega_{b,m}^2 - \omega^2\right)$ with $M_m^b$ the modal mass and $\omega_{b,m}$ the natural frequency of the uncoupled subsystem *b*. Hysteretic damping can be introduced by making the stiffness matrix complex. The corresponding generalised external and interface forces of the *m*th mode are

$$F_{e,m} = \int_{D_b^e} f_e(\mathbf{x}_b^e)\phi_m^b(\mathbf{x}_b^e)d\mathbf{x}_b^e; \quad F_{i,m}^b = \int_{D_b^i} f_i^b(\mathbf{x}_b^i)\phi_m^b(\mathbf{x}_b^i)d\mathbf{x}_b^i \tag{3, 4}$$

where $D_b^e$ and $D_b^i$ are the respective domains where the external force is applied and the interface force occurs and $\mathbf{x}_b^e$ and $\mathbf{x}_b^i$ are the corresponding local coordinates.

In a similar manner, the displacement $w_p$ of subsystem *p* is given by

$$w_p(\mathbf{x}_p) = \sum_r \psi_r^p(\mathbf{x}_p)\, q_r^p(t) \tag{5}$$

where $\mathbf{x}_p$ is the local coordinate vector of the subsystem $p$ and $\psi_r^p$ is the $r$th mode shape. Similar to subsystem $b$, the modal solution of the system $p$ can be found as

$$\mathbf{q}_p = \mathbf{S}_p^{-1}\mathbf{F}_i^p \tag{6}$$

where $\mathbf{S}_p$ is a diagonal matrix of modal dynamic stiffnesses of the form $S_r^p = M_r^p\left(\omega_{p,r}^2 - \omega^2\right)$ with $M_r^p$ the modal mass of subsystem $p$. The generalised interface force is

$$F_{i,r}^p = \int_{D_p^i} f_i^p(\mathbf{x}_p^i)\psi_r^p(\mathbf{x}_p^i)d\mathbf{x}_p^i \tag{7}$$

where $D_p^i$ is the interface domain and $\mathbf{x}_p^i$ is the local coordinate where the interface force occurs in subsystem $p$. When coupling systems $b$ and $p$, the interface domains $D_b^i$ and $D_p^i$ will be equal.

## 2.2. Structural response based on the general modal coupling

Consider the interface force $f_i$ applied at interface local coordinate $\mathbf{x}_i$ and the corresponding displacement at $\mathbf{x}_i$, $w_i(\mathbf{x}_i)$. This force and displacement can be presented in terms of a complete set of orthogonal basis functions, $\chi_k(\mathbf{x}_i)$ spanning the interface domain, as

$$f_i(\mathbf{x}_i) = \sum_k \chi_k(\mathbf{x}_i)F_{i,k}\,; \qquad w_i(\mathbf{x}_i) = \sum_k \chi_k(\mathbf{x}_i)q_{i,k} \tag{8, 9}$$

where $F_{i,k}$ is the $k$th generalised interface force and $q_{i,k}$ is the $k$th generalised interface coordinate. Such expressions for the force and displacement can be utilised for a general coupling situation, for example, when the mode shape functions of the subsystems are different and their interaction through the interface needs to be identified.

The motion of the coupled system can be described in terms of the force equilibrium and the continuity of the displacement through the interface, which are

$$f_i(\mathbf{x}_i) = f_i^b(\mathbf{x}_b^i) = f_i^p(\mathbf{x}_p^i)\,; \qquad w_i(\mathbf{x}_i) = w_b(\mathbf{x}_b^i) = w_p(\mathbf{x}_p^i). \tag{10, 11}$$

Combining equations (4), (8) and (10) results in

$$\mathbf{F}_i^b = \boldsymbol{\beta}_b\mathbf{F}_i \tag{12}$$

where $\mathbf{F}_i^b$ and $\mathbf{F}_i$ are the interface force matrices respectively given in the local coordinate of subsystem $b$ and the interface local coordinate and the matrix of factors $\boldsymbol{\beta}_b$ is given by

$$\beta_{mk}^b = \int_{D_b^i} \phi_m^b(\mathbf{x}_b^i)\chi_k(\mathbf{x}_i)d\mathbf{x}_b^i\,. \tag{13}$$

Thus, $\boldsymbol{\beta}_b$ is a matrix of modal correlations between the modes of subsystem $b$ and the basis functions of the interface. Then equation (2) becomes

$$\mathbf{q}_b = \mathbf{S}_b^{-1}\left(\mathbf{F}_e^b - \boldsymbol{\beta}_b\mathbf{F}_i\right). \tag{14}$$

Similarly, combining equations (7), (8) and (10) gives

$$\mathbf{F}_i^p = \boldsymbol{\beta}_p \mathbf{F}_i \tag{15}$$

where

$$\beta_{rk}^p = \int_{D_p^i} \psi_r^p(\mathbf{x}_p^i)\chi_k(\mathbf{x}_i)d\mathbf{x}_p^i . \tag{16}$$

Thus equation (6) becomes

$$\mathbf{q}_p = \mathbf{S}_p^{-1}\boldsymbol{\beta}_p \mathbf{F}_i . \tag{17}$$

As continuity should hold at the interface, equation (11),

$$\sum_m \phi_m^b(\mathbf{x}_b^i)q_m^b = \sum_r \psi_r^p(\mathbf{x}_p^i)q_r^p = \sum_k \chi_k(\mathbf{x}_i)q_k^i . \tag{18}$$

Multiplying this by $\chi_k(\mathbf{x}_i)$ and integrating over the interface using equations (13) and (16) gives the relationship between the individual subsystem generalised coordinates as

$$\boldsymbol{\beta}_b^T \mathbf{q}_b = \boldsymbol{\beta}_p^T \mathbf{q}_p . \tag{19}$$

### 2.3. Special case using beam functions as basis functions

Taking the special case where the beam mode shapes of subsystem *b* can be used as the interface basis functions

$$\chi_k = C_k \phi_k^b \tag{20}$$

for some normalisation constant $C_k$ chosen to ensure

$$\boldsymbol{\beta}_b = \mathbf{I} . \tag{21}$$

Such a special case can be realised, for example, when a beam is attached at the edge of a rectangular plate, where the edge motion is described using the beam mode shape functions and consequently a different basis function is not necessary for the interface. Thus, the above equations (14), (17) and (19) can be simplified. The system response in terms of $\mathbf{q}_p$ becomes

$$\mathbf{q}_p = \left(\mathbf{S}_p + \boldsymbol{\beta}_p \mathbf{S}_b \boldsymbol{\beta}_p^T\right)^{-1} \boldsymbol{\beta}_p \mathbf{F}_e^b = \mathbf{S}^{-1}\mathbf{F} , \tag{22}$$

where $\mathbf{F} = \boldsymbol{\beta}_p \mathbf{F}_e^b$ is the generalised force vector in plate modal coordinates and $\mathbf{S}$ is a combined dynamic stiffness matrix. Hence the response of subsystem *b* is

$$\mathbf{q}_b = \boldsymbol{\beta}_p^T \left(\mathbf{S}_p + \boldsymbol{\beta}_p \mathbf{S}_b \boldsymbol{\beta}_p^T\right)^{-1} \boldsymbol{\beta}_p \mathbf{F}_e^b = \boldsymbol{\beta}_p^T \mathbf{S}^{-1}\mathbf{F} . \tag{23}$$

The dynamic stiffness matrix in equation (22) can be assembled in terms of modal mass and stiffness matrices

$$\mathbf{S} = \mathbf{K}_p + \boldsymbol{\beta}_p \mathbf{K}_b \boldsymbol{\beta}_p^T - \omega^2 \mathbf{M}_p - \omega^2 \boldsymbol{\beta}_p \mathbf{M}_b \boldsymbol{\beta}_p^T \tag{24}$$

where $\mathbf{K}_p$ and $\mathbf{M}_p$ are diagonal matrices consisting of terms $K_{p,r} = \omega_{p,r}^2 M_{p,r}$ and $K_{b,m} = \omega_{b,m}^2 M_{b,m}$ . Note that $\mathbf{M} = \mathbf{M}_p + \boldsymbol{\beta}_p \mathbf{M}_b \boldsymbol{\beta}_p^T$ is an assembled mass matrix and $\mathbf{K} = \mathbf{K}_p + \boldsymbol{\beta}_p \mathbf{K}_b \boldsymbol{\beta}_p^T$ is the corresponding stiffness matrix. Whilst the individual matrices $\mathbf{K}_p, \mathbf{K}_b, \mathbf{M}_p$ and $\mathbf{M}_b$ are diagonal the assembled dynamic stiffness matrix is not due to coupling through the interface.

## 3. A modal formulation for the coupled motion of a system of four beams attached to a plate

The coupling method described above is now applied to investigate the motion of a framed structure consisting of four beams and a rectangular plate of dimensions $L_x \times L_y$, as shown in Figure 2. It can be described in terms of the mode shapes of the individual components; the coupling can be described based on the modal coordinates of the plate. It is not necessary to obtain the modes of the coupled structure itself because the relevant separate modal matrices of the uncoupled structures are used, as presented in Section 2.

It is convenient to assume that the beams are infinitely stiff to torsion, and correspondingly, all edges of the plate are assumed to be 'sliding' (i.e. no rotational displacement along the plate edge), which significantly reduces the complexity of the analytical and numerical analyses. This assumption may be justified, if the beams have large cross section and they are connected at right angles to give a framed structure, although small discrepancies may be found compared with experimental results. A separable solution can be used for the plate and the two sets of functions in the $x$ and $y$ directions are identical to the beam shape functions. For simplicity, the beams are assumed to be attached to the plate along their respective neutral axes.

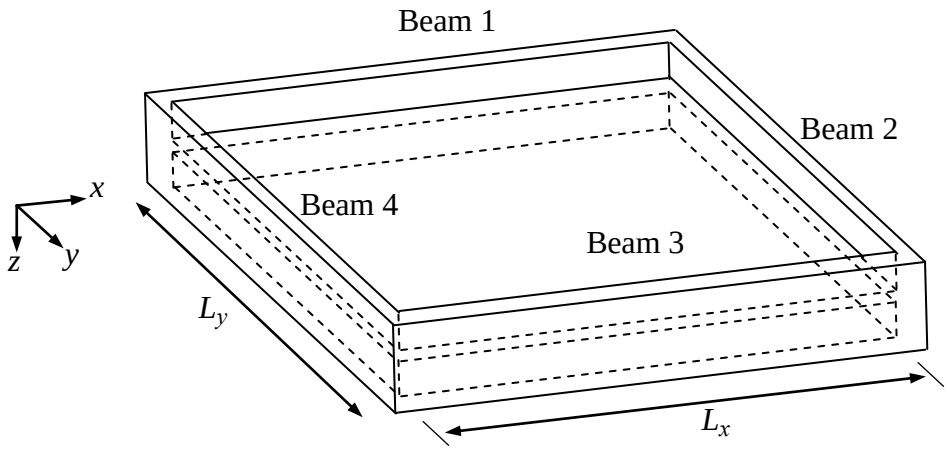


Figure 2. The coupled structure consisting of four beams and a rectangular plate. The beams are attached to the plate along their respective neutral axes.

### 3.1. A modal description for flexural beam and plate vibration

The flexural displacement of a plate having an arbitrary shape can also be represented using an infinite series as in equation (5). Limiting the plate to a rectangular shape, its mode shapes can be represented by combination of shape functions in the two perpendicular directions. Thus, the mode shape of the rectangular plate $\psi_r(x, y)$ can be expressed as the product of two separable functions so that each depends on a single spatial variable $x$ or $y$ i.e.

$$\psi_r^p(x,y) = \phi_{m_r}(x)\phi_{n_r}(y) = \phi_{m_r}\phi_{n_r} \tag{25}$$

where $\phi_{m_r}(x)$ and $\phi_{n_r}(y)$ are selected as two linearly independent sets satisfying all of the appropriate boundary conditions. If all edges of the rectangular plate have sliding boundary conditions, then the corresponding separable functions are exact and are identical to the beam mode shape functions. They are given by

$$\phi_{m_r} = \cos k_x x\,,\ \phi_{n_r} = \cos k_y y \tag{26}$$

where

$$k_x = m_r\pi/L_x \ \text{ for } \ m_r = 0,1,2,\cdots; \qquad k_y = n_r\pi/L_y \ \text{ for } \ n_r = 0,1,2,\cdots, \tag{27}$$

$L_x$ and $L_y$ are the length of the beams in the directions $x$ and $y$. The cases $m_r = 0$ and $n_r = 0$ correspond to the rigid body modes. Separable solutions also exist for simply supported boundaries.

### 3.2 A modal method for the framed structure

The flexural motion of the framed structure can be derived using the mode shapes $\psi_r$ (satisfying boundary conditions) of the uncoupled plate as presented in Section 3.1 and generalised coordinates $q_r$ as given in equation (5) [20].

Due to continuity at the plate edges the flexural displacement of the beams shown in Figure 2 is given by

$$\begin{aligned} w_{b1}(x) &= w_p(x,0);\ \ w_{b3}(x) = w_p(x,L_y) \\ w_{b4}(y) &= w_p(0,y);\ \ w_{b2}(y) = w_p(L_x,y) \end{aligned} \tag{28}$$

The generalised mass matrix of the coupled structure is found, in a similar way to Section 2.2 and also given in [7], to be

$$\mathbf{M} = \mathbf{M}_p + \boldsymbol{\beta}_1\mathbf{M}_{b1}\boldsymbol{\beta}_1^T + \boldsymbol{\beta}_2\mathbf{M}_{b2}\boldsymbol{\beta}_2^T + \boldsymbol{\beta}_3\mathbf{M}_{b3}\boldsymbol{\beta}_3^T + \boldsymbol{\beta}_4\mathbf{M}_{b4}\boldsymbol{\beta}_4^T \tag{29}$$

where $\mathbf{M}_{bj}$ is the diagonal modal mass matrix of beam $j$ and $\boldsymbol{\beta}_j$ are diagonal matrices consisting of the terms

$$\begin{aligned} \beta_1 &= C_k\int_0^{L_x}\phi_{m_r}(x)\phi_{n_r}(0)\phi_k(x)dx = \delta_{m_r k}, \\ \beta_2 &= C_l\int_0^{L_y}\phi_{m_r}(L_x)\phi_{n_r}(y)\phi_l(y)dy = \delta_{n_r l}(-1)^{m_r}, \\ \beta_3 &= C_k\int_0^{L_x}\phi_{m_r}(x)\phi_{n_r}(L_y)\phi_k(x)dx = \delta_{m_r k}(-1)^{n_r}, \\ \beta_4 &= C_l\int_0^{L_y}\phi_{m_r}(0)\phi_{n_r}(y)\phi_l(y)dy = \delta_{n_r l}, \end{aligned} \tag{30}$$

where $\phi_k(x) = \cos(k\pi x/L_x)$, $\phi_l(y) = \cos(l\pi y/L_y)$ and

$$C_k = 1/L_x \ \text{ for } k = 0; \quad 2/L_x \ \text{ for } k \geq 1, \tag{31}$$

$$C_l = 1/L_y \ \text{ for } l = 0; \quad 2/L_y \ \text{ for } l \geq 1, \tag{32}$$

where $m$, $k$ are the order numbers (numbers of half wavelengths) of the separable function (i.e. beam mode shape function) in the $x$ direction and $n$, $l$ are the same in the $y$ direction for mode $r$.

Similarly the generalised stiffness matrix is given by

$$\mathbf{K} = \mathbf{K}_p + \boldsymbol{\beta}_1 \mathbf{K}_{b1} \boldsymbol{\beta}_1^T + \boldsymbol{\beta}_2 \mathbf{K}_{b2} \boldsymbol{\beta}_2^T + \boldsymbol{\beta}_3 \mathbf{K}_{b3} \boldsymbol{\beta}_3^T + \boldsymbol{\beta}_4 \mathbf{K}_{b4} \boldsymbol{\beta}_4^T \tag{33}$$

where $\mathbf{K}_p$ is a diagonal matrix with $K_{p,r} = \omega_{p,r}^2 M_{p,r}$ and $K_{bj,m} = \omega_{bj,m}^2 M_{bj,m}$.

It is assumed that the force is applied to beam 1, so that the generalised force in plate modal coordinates is given by

$$\mathbf{F} = \boldsymbol{\beta}_1 \mathbf{F}_{b1} \tag{34}$$

where $\mathbf{F}_{b1}$ is the generalised force in the modal coordinates of beam 1 given by $F_{b1,m} = F_0 \phi_m(x_1)$ for a point force $F_0$ in the $z$ direction, applied at $x = x_1$ on beam 1. The response in generalised coordinates is found from equation (22) and used in equation (5) to find the flexural displacement of the framed structure. The numerical results based on the modal approach follows in Section 6, with comparison with the approximate wave model which is described next.

## 4. Wave model of a frame consisting of four beams

Before considering a wave model of the beam-plate coupled system, a rectangular frame structure consisting of four beams only is considered, as shown in Figure 3. The exact response of this system can be found using a wave approach. The beams are assumed to have identical cross-sections. For harmonic motion at frequency $\omega$, each beam carries free flexural waves with wavenumber $\tilde{k}_b^4 = m_b' / \tilde{D}_b \omega^2$ where $m_b'$ is the beam mass per unit length and $\tilde{}$ is used for complex quantities. An external force is applied at the corner of beams 1 and 4. Each beam is assumed to be infinitely stiff to torsion. Damping is introduced through a complex bending stiffness $\tilde{D}_b$.

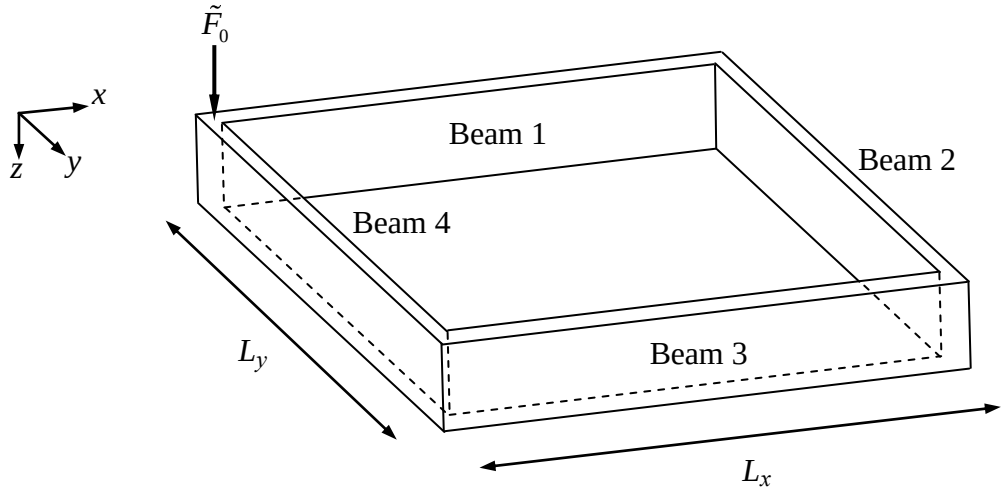


Figure 3. Frame wave model consisting of four beams.

The displacement of each beam can be given by an equation of the following form, for example for beam 1 (assuming time-harmonic motion with dependence $e^{i\omega t}$):

$$\tilde{w}_1(x) = \tilde{A}_{11}e^{-i\tilde{k}_x x} + \tilde{A}_{12}e^{-\tilde{k}_x x} + \tilde{A}_{13}e^{i\tilde{k}_x x} + \tilde{A}_{14}e^{\tilde{k}_x x}. \quad (35)$$

where $\tilde{A}_{1i}$ are the amplitudes of the corresponding flexural waves with wavenumber $\tilde{k}_x$. The external force applied at the corner of beams 1 and 2 should be included in the force equilibrium condition.

Therefore, the boundary conditions for the four-beam structure shown in Figure 3 are:
(i) Continuity equation; equal displacement at corners (4 boundary conditions)
(ii) No rotation at the ends of the beams (8 boundary conditions)
(iii) Force equilibrium at the corners (4 boundary conditions)

Then, the equation of motion can be written in a matrix form.

$$\mathbf{F} = \mathbf{K}\mathbf{A} \quad (36)$$

The displacement vector **A** consists of 16 coefficients of each wave in the beam equations, such as equation (35). The force vector **F** (16 elements including the external force term) and the frame dynamic stiffness matrix **K** (16 by 16) are obtained by substituting the response of the form of equation (35) into the boundary conditions presented above. The displacement of any beam of the coupled structure shown in Figure 3 can be found from:

$$\mathbf{A} = \mathbf{K}^{-1}\mathbf{F} \quad (37)$$

allowing $\tilde{w}_i(x)$ to be found from equation (35). The results will be shown in Section 6.

## 5. Analysis of a four-beam-plate coupled system using a wave approach

### 5.1 Wave approach

A wave method [1] is extended to the particular situation considered, so that the force is applied to a stiff beam and a plate acts as an impedance to the beam. Therefore, flexural vibration energy is transferred from the beam to the plate. To analyse the framed structure shown in Figure 2 using a wave approach, the plate is represented by a line impedance attached to each beam from which the coupled beam wavenumber can be determined. The method for obtaining the wavenumber is described in [1,2] and summarised here. Strictly, even if the plate is very flexible, connecting the plate to the stiff beams has an influence on the motion of the coupled structure. This is clearly the case for low frequency motion especially at corners. However, the two edges of the plate cannot connect two beams in the wave model. Therefore, this method is only applicable for mid- and high frequency regions, in which the global motion is governed by the stiff beams and the flexible plate acts as an impedance added to those beams. This method is an approximate method, but it is very compact and fast compared to a modal method or FEM because only the governing waves in the systems are considered.

Consider a single beam lying parallel to the *x* axis with a plate attached on one side. Strictly, in such a coupled system consisting of stiff beams and a flexible rectangular plate, multiple plate waves occur in the *x* direction (i.e. beam direction); however, it is shown in [3] that if the system is excited on one of the beams, the response on the plate and the driven beam is dominated by the waves with a wavenumber component in the *x*

direction that is close to that of the driven beam. Therefore, the dynamic motion of a beam-plate coupled system can be modelled with wavenumber trace matching. The most important hypothesis in the wave method is that the beam coupled to a plate is sufficiently stiffer than the plate so that the beam wavenumber should be sufficiently smaller than the plate free wavenumber ( $k_p >> k_b$ ).

Assuming the beam is infinitely stiff to torsion, the effect of the plate attached to the beam can be represented approximately by a wave impedance of the damped plate. For a wavenumber $\tilde{k}_x$ in the beam this is given by [2]:

$$\tilde{Z}'_p \approx \frac{\tilde{D}_p 2\tilde{k}_p^3}{\omega}\left[\frac{1-\tilde{\beta}_y\tilde{r}}{(1+\tilde{\beta}_y\tilde{r})-i(1-\tilde{\beta}_y\tilde{r})}\right] \tag{38}$$

where $i$ is the imaginary unit, $\tilde{D}_p$ is the complex plate bending stiffness, $\tilde{k}_p$ is the free plate wavenumber, $\omega$ is the frequency, $\tilde{\beta}_y = e^{-i\tilde{k}_y 2L_y}$ allows for the propagation and wave attenuation in the plate, $\tilde{k}_y$ is the trace plate wavenumber in the $y$ direction (which depends on $\tilde{k}_x$) and $\tilde{r}$ is the reflection coefficient dependent on the boundary conditions of the opposite edge ( $y = L_y$ ). For a sliding condition, $\tilde{r} = 1$.

If the plate is infinitely wide so that $L_y = \infty$, then the approximate impedance of the plate reduces to:

$$\tilde{Z}'_p \approx \frac{\tilde{D}_p\tilde{k}_p^3}{\omega}(1+i) = \frac{m''_p\omega}{\tilde{k}_p}(1+i). \tag{39}$$

where $m''_p$ is the plate mass per unit area. The general dispersion equation for the waves in the beam coupled to a plate is given by [1,2]:

$$\tilde{D}_b\tilde{k}_x^4 = m'_b\omega^2 - i\omega\,\tilde{Z}'_p \tag{40}$$

where $\tilde{D}_b$ is the complex beam bending stiffness and $\tilde{k}_x$ is the coupled beam wavenumber. As the impedance in equation (38) includes the plate trace wavenumber $\tilde{k}_y$, $\tilde{k}_y$ will be obtained from the trace wavenumber relationship, $k_y = \sqrt{k_p^2 - k_x^2}$. Then, an iterative method is required to find an improved estimate for the wavenumber $\tilde{k}_x$ in solving equations (40) and (38). There are multiple solutions [3] but the one closest to the free beam wavenumber is sought using Muller's method [2]. Once the coupled beam wavenumber is found, the motion of the finite beam possessing the coupled wavenumber can be represented by:

$$\tilde{w} = \tilde{A}_1 e^{-i\tilde{k}_x x} + \tilde{A}_2 e^{-\tilde{k}_x x} + \tilde{A}_3 e^{i\tilde{k}_x x} + \tilde{A}_4 e^{\tilde{k}_x x} \tag{41}$$

where $\tilde{A}_1$ and $\tilde{A}_3$ are the amplitudes of travelling waves, $\tilde{A}_2$ and $\tilde{A}_4$ are the amplitudes of the nearfield waves and $\tilde{k}_x$ is the complex travelling wavenumber in the coupled beam.

### 5.2 Coupled structure consisting of four beams: application of the wave method

If it can be assumed that most of the power transferred to the plate is dissipated there and only a small fraction of the power is transferred to other beams, then the framed structure consisting of four beams and the rectangular plate (Figure 2) can be represented by a system consisting of the four beams, each having the coupled wavenumber due to the plate impedance. Then, such a system can be easily modelled using the wave method. The structure physically satisfying the above assumption is shown in Figure 4. The external force is applied at the corner of beam 1 and beam 4. The downward arrows mean that beams 1, 2, 3 and 4 are connected at the corners. Each plate is exclusively attached to the individual beam. This implies that each plate is acting upon the corresponding beam as an impedance. As sliding edges are assumed in the framed structure in Figure 2, the same sliding boundary conditions are used at the opposite edges of the plate for the structure shown in Figure 4. This may result in different responses compared with those of the framed structure, as the opposite edges should in fact be attached to other beams. In particular, the responses of the opposite beam are probably different because this beam is physically separated from the plate, and consequently, any fraction of energy from the plate cannot be transferred; however, it is expected that the energy level estimates of the driven beam and the receiving plate are reasonable, as the wave model properly explains the relationship between the driven beam and the energy-receiving plate.

The method for obtaining the response using the wave model is similar to that given in Section 4. The excitation force is also defined in the same manner at the corner. Due to the attached plates, the free beam wavenumber $\tilde{k}_b$ is replaced by the coupled wavenumber obtained from equation (40) in Section 5.1. The boundary conditions are the same as in Section 4. The validity of this wave model will be assessed in the next sections of the paper.

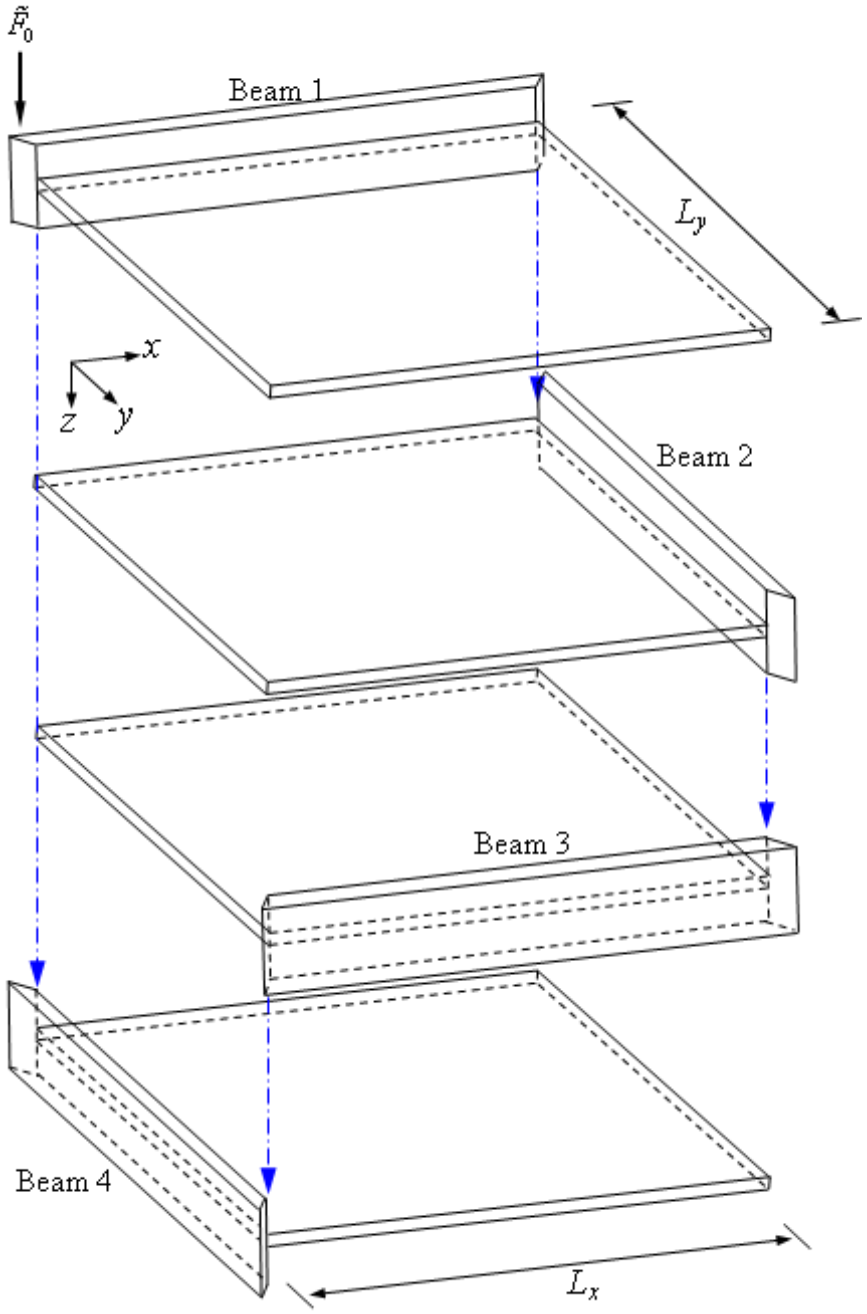


Figure 4. Configuration of the coupled structure for the use of the wave method.

## 6. Results

### 6.1 Configuration of framed structure

The numerical simulations based on the modal and wave methods are presented and compared in this section. The material properties and dimensions of the coupled structure are given in Table 1. The ratio of the free wavenumbers of the plate and beam

$k_p/k_b$ is equal to 3.18, which is large enough to apply the wave method [2,1]. A wide frequency range from 5.6 to 1412 Hz (one-third octave bands 6.3 to 1250 Hz) is considered and 19 frequency data points are used in each one-third octave band to give an average value. In this frequency range each beam has between 7 and 9 modes so that the beams can be considered to be in their 'low frequency' range. The plate has a modal density of about 0.4 modes per Hz, so that its 10th mode occurs by about 23 Hz and about 500 modes can be expected below 1412 Hz. The modal overlap factor [2] is the ratio of the half-power bandwidth to the average frequency spacing between adjacent natural frequencies. If it is greater than unity, the system can be considered to have 'high frequency' behaviour. The modal overlap factor of the plate is greater than unity above about 50 Hz. This plate, therefore, has 'high frequency' behaviour over much of the frequency range considered.

Table 1. Material properties and dimensions of the coupled structure shown in Figure 2.

| Material | Perspex | Beam length, $L_x$ (m) | 1.0 |
|---|---|---|---|
| Young's modulus, $E$ ($GNm^{-2}$) | 4.4 | Height of beam, $h$ (mm) | 22.0 |
| Poisson's ratio, $\nu$ | 0.38 | Beam thickness, $b$ (mm) | 6.0 |
| Density, $\rho$ ($kgm^{-3}$) | 1152.0 | Plate width, $L_y$ (m) | 0.75 |
| Damping loss factor, $\eta_b$, $\eta_p$ | 0.05 | Plate thickness, $t_p$ (mm) | 2.0 |

The wave approach is approximate, and its results are compared here with those from the modal method. For the latter, convergence has been examined, and the highest mode number in each direction is chosen to be 50, which provides an accurate response (maximum error of less than 0.18% in the current frequency range [10]). Thus more than twice as many modes are included in each direction than are contained in the frequency range of interest.

### 6.2 Mobilities

To understand the dynamic characteristics of the system, the mobility (velocity response to a unit input force) is investigated. Initially, in Figure 5, the point mobilities of the beam framework with and without the added plates, i.e. the structures of Figures 3 and 4, are compared so that the effect of the plates can be illustrated. Many more resonance peaks are observed when the plates are attached, due to the coupling with plate modes; however, it can also be seen that (i) the average vibrational level decreases significantly and (ii) the height of the peaks and troughs is reduced. This is because the plate behaves like mass and damping attached to the beam [1,2].

An asymptotic representation for these point mobilities is useful in understanding the effect of the plate. This can be obtained by making two adjacent beams semi-infinite in the structures shown in Figures 3 and 4; the other two beams are in fact removed. The point mobility is given by:

$$\tilde{Y}_0 = \frac{(1-i)\omega}{4\tilde{D}_b \tilde{k}_b^3} \tag{42}$$

which is equal to the result for an infinite beam (due to the sliding condition at the joint). The effect of the semi-infinite plate coupled to the beams can be realised by replacing $\tilde{k}_b$ in equation (42) by the coupled beam wavenumber $\tilde{k}_x$, which is obtained in equations (39) and (40). In such a situation, the two plates coupled to beams 1 and 4 in Figure 4 are infinite in their respective width direction. It is expected that equation (42) with $\tilde{k}_x$ obtained from the semi-infinite plate represents the asymptotic point mobility of the four-beam-plate structure.

These asymptotic results for the point mobilities are also shown in Figure 5 (dotted and dot-dash lines). They represent the general tendency of the corresponding point mobilities very well. The addition of the coupled plate reduces the response level because of the added mass effect; however, this effect decreases with increasing frequency as the added mass due to the plate reduces as its wavelength reduces.

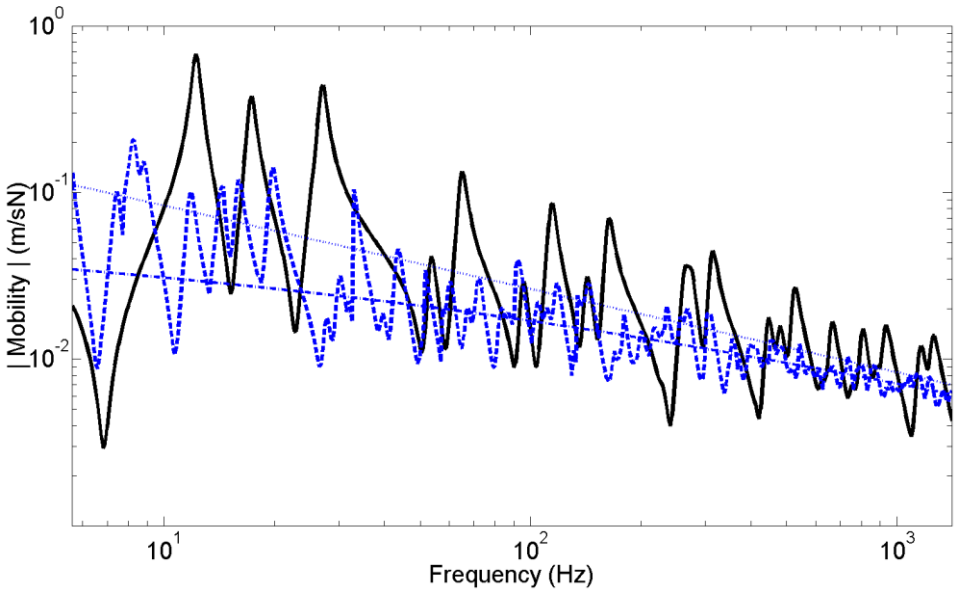


Figure 5. Point mobility comparison of the plate-coupled structure as in Figure 4 and the structure consisting of only four beams as in Figure 3 (based on the wave method, excitation at ($x$,$y$) = (0,0)). - - —, frame without plates; ·····, two semi-infinite beams without plates; ———, frame coupled to finite plates; —·—·—, two semi-infinite beams coupled to semi-infinite plates.

The point mobility of the coupled system from the wave method is compared with the point mobility predicted by the modal method in Figure 6. It can be seen that at high frequencies, the results are in good agreement in terms of general level, although at lower frequencies there are detailed differences between the two methods. This will be discussed later in Section 6.3.

It is also interesting to compare these point mobilities with those obtained when semi-infinite plates are assumed to be connected to the beam framework. The semi-infinite plate is realised by allowing the width of the plates shown in Figure 4 to become infinite, and the corresponding wavenumber can be found using equation (39) instead of equation

(38) in equation (40). It can be seen that the point mobilities in Figure 6 oscillate around the result obtained using the semi-infinite plates. The damping added to the beams increases considerably when the semi-infinite plate is introduced, resulting in a behaviour of the coupled structure similar to a heavily damped beam. It is known that an attached plate with a short wavelength behaves like a mass and damping on a beam possessing a long wavelength, such an arrangement acting like a fuzzy structure [21].

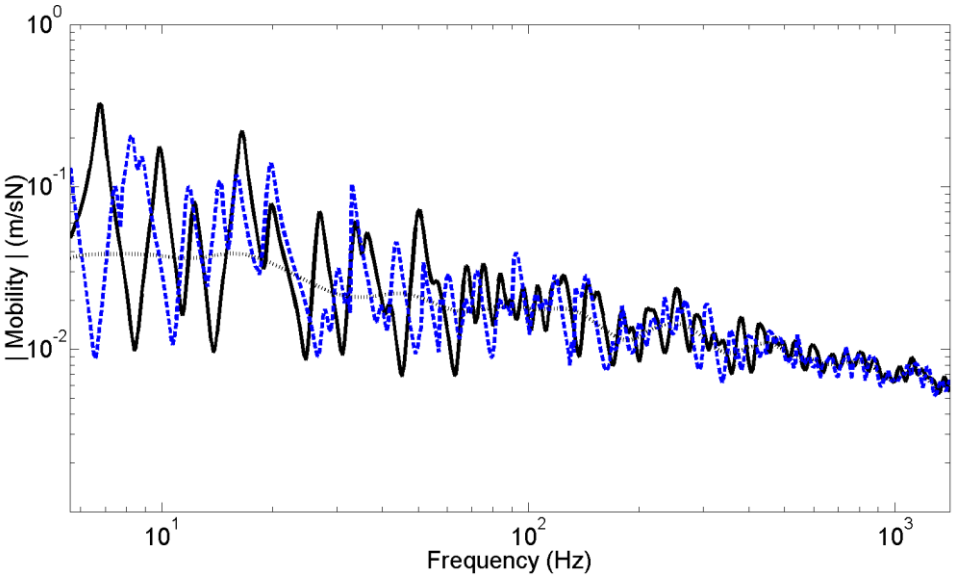


Figure 6. Point mobilities of the coupled structure as in Figure 4 based on the wave method and the modal method (excitation at $(x,y) = (0,0)$). - - —, modal method; ———, wave method (finite plates); ·····, wave method (semi-infinite plates).

### 6.3 Power investigation

In this section, the powers transferred and dissipated in each subsystem are compared. First, the power transferred from the beams to the plate, equal to the dissipated power in the plate, is investigated. The power transferred from the beam to the plate is calculated by integrating $\mathrm{Re}\left\{ \tilde{f}_i(x)^* \tilde{v}_i(x) \right\}/2$ along the interface $i$, where $\tilde{v}_i(x) = i\omega \tilde{w}_i(x)$ is the velocity response of the coupled beam and * means complex conjugate. The force acting on the plate from the beam along the interface $i$ is given by:

$$\tilde{f}_i(x) = \tilde{v}_i(x) \tilde{Z}'_p \qquad (43)$$

For the wave method, the power transferred is the sum over all four attached plates, and similarly, the plate energy is found from the sum of the energy in each plate in the model. The input power, for a unit force, is calculated from $\mathrm{Re}\left\{ \tilde{Y}_0 \right\}/2$ (see equation (42)).

In Figure 7, the power transferred to the plate, obtained using the modal and wave methods is compared. Since the exact location of resonance peaks is of less interest than a frequency band average result when considering the mid-frequency region, these results are shown in terms of one-third octave band averages. The results from the two methods agree quite well, especially at high frequencies, although the wave method

gives a lower result than the modal method. The differences below about 60 Hz may occur because of differences between the global modes of the structure shown in Figure 4, assumed for the wave method, and those of the actual framed structure used in the modal method (Figure 2). Thus, the assumptions used for the wave method do not appear to be appropriate for calculating the low frequency response or the subsequent coupling power.

The average values from the modal method are also compared with the result from the wave method in which attached semi-infinite plates are considered. A very good agreement can be observed at high frequencies. These results imply that the average power transfer is hardly influenced by changes in the plate width, if the flexible plate acts as an impedance to the beam.

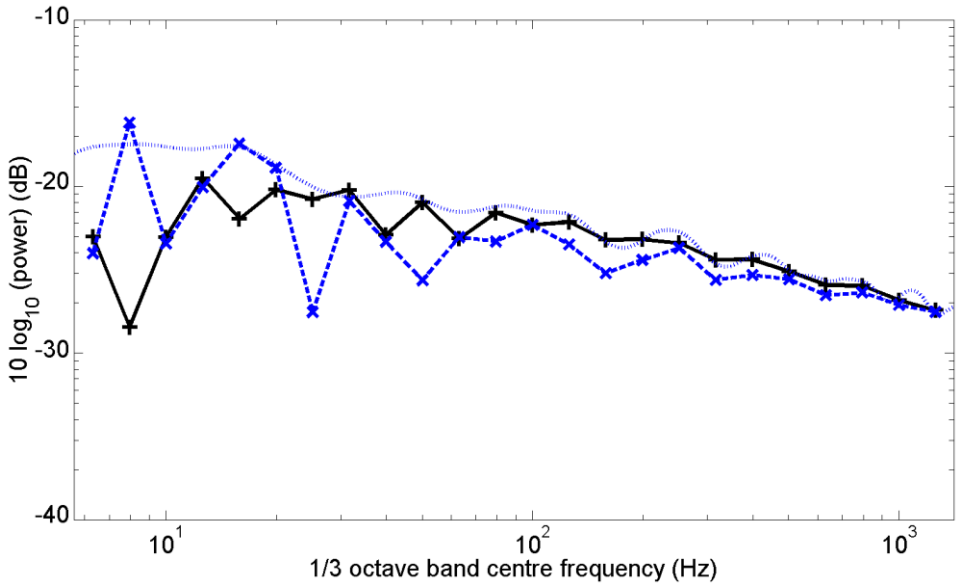


Figure 7. Power transfer from four beams to the plate in one-third octave bands (point force is applied at $x = 0$). —+—, modal method; −×−, wave method (finite plates); ·····, wave method (semi-infinite plates).

The power transfer from the four beams to the plate normalised by the power input of the excitation is shown for the two methods in Figure 8. Even though it was expected that the power transfer of the wave model is an underestimate, it can be seen that the ratios based on the wave method and the modal method are in reasonable agreement above about 50 Hz. This means that the fully framed structure can be analysed in terms of power transfer estimates using the wave method in the mid-frequency region; however, there are large differences at low frequencies. This indicates that the wave model is not suitable to represent the framed structure at low frequencies.

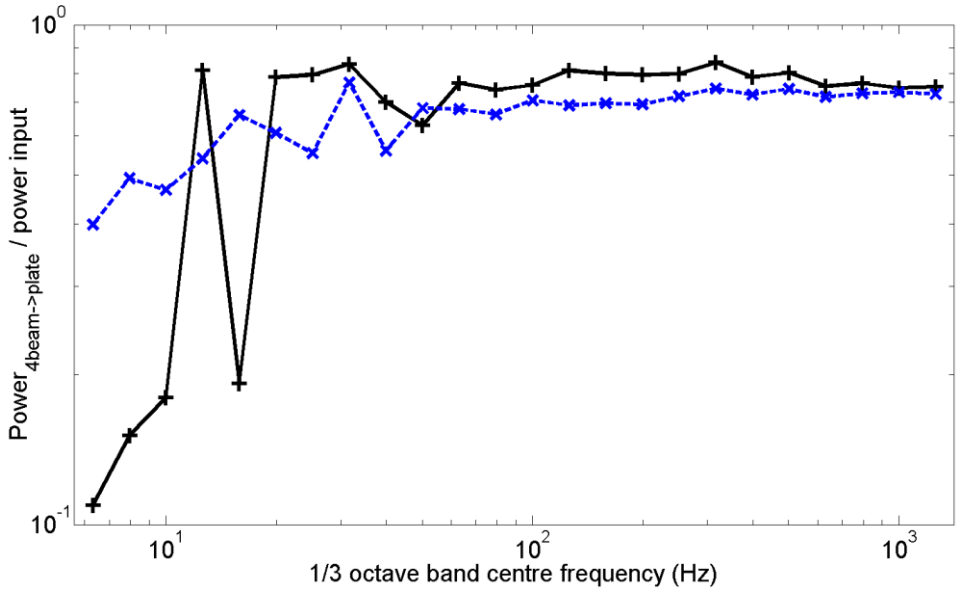


Figure 8. Power ratio (of power transfer from the four beams to the plate to the power input) based on the modal method and the wave method in a one-third octave band average (point force is applied at $x = 0$ of beam 1). $-\cdot+\cdot-$, modal method; $-\times-$, wave method (finite plates).

Finally, the power dissipated in each subsystem is investigated. It can be expected that the power dissipated in each beam is small in comparison with the power dissipated by the plate. The results based on the modal model are shown in Figure 9. The power dissipated in the plate can be seen to be larger than the others by at least a factor of 10 (10 dB) above 20 Hz. It may also be noted that beams 2 and 3 have lower dissipated powers than beams 1 and 4, particularly above about 100 Hz. The excitation is located at the junction of beams 1 and 4, so the power is directly transmitted to these beams, whereas the power transferred from beam 1 to beam 2 and from beam 4 to beam 3 passes through one junction, which may cause some attenuation.

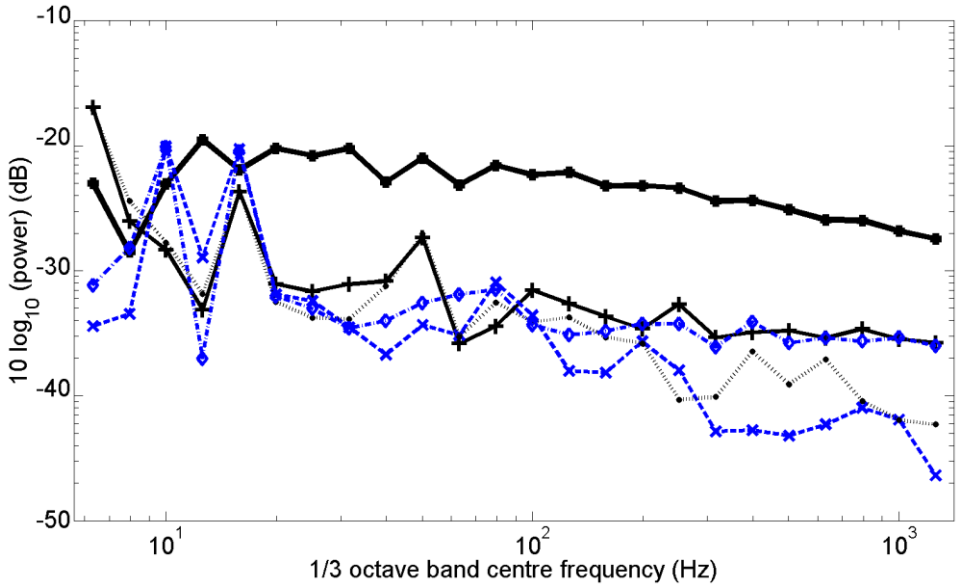


Figure 9. Power dissipated in each subsystem in one-third octave bands for the four-beam-plate system. Based on the modal method. —+—, plate; - -+- , beam 1; −×−, beam 2; ···•···, beam 3; ·−◇·−, beam 4.

## 7. Experimental study

Experimental studies have been carried out for the validation of the analytical models described. The power input obtained experimentally is compared with the numerical predictions using the various models.

Whereas sliding boundaries were applied in the numerical analyses for convenience, in the experiments, the boundaries are free. Consequently, the comparisons of the quantities, such as the mobilities, between the models and experiments, are not expected to give good agreement due to changes in the resonance frequencies. Therefore the measured results are expressed in terms of kinetic energies, and the ratio of energies in various components relative to that in the excited beam are compared with those obtained from the models. Moreover, these results are expressed in terms of one-third octave band averages to assist with comparisons in which exact resonance frequencies do not match and indeed are not of direct interest.

### 7.1 Experimental models and configurations

Each coupled system consists of a rectangular plate and four beams that are made of acrylic plastic. The specific dimensions are as listed in Table 1. In each case, the plate has a thickness of 2 mm and dimensions of $1.0\times0.75$ m. Strips of a width of 6 mm were fixed above and below the 2 mm plate to form beams, which are symmetric at the plate centreline. Coupled structures denoted F1 (four similar beams) and F2 (dissimilar beams) have been studied. The averaged dimensions and the maximum tolerances of the beams for the different structures are presented in Table 2. The numbering of the four beams corresponds to Figures 2 and 10. Note that for the beam dimensions considered, the ratio of the free plate wavenumber to the coupled beam wavenumber $k_p/k_x$ is at least 2.

Material properties, including damping, were measured [2] and used in the corresponding calculations.

Table 2. Nominal dimensions of coupled systems used in the measurements.

| Sample No. | Beam height and width (mm) | | | | | Comments |
|---|---|---|---|---|---|---|
| | $h_1$ | $h_2$ | $h_3$ | $h_4$ | $b$ | |
| F1 | 23.6 ± 0.86 | | | | 6.1 ± 0.11 | Similar beams |
| F2 | 24.1 ± 0.36 | 13.3 ± 1.11 | 13.3 ± 1.11 | 24.1 ± 0.36 | 6.0 ± 0.41 | Dissimilar beams |

Figure 10 shows a photograph of the experimental configurations in which the coupled system was suspended, and an exciter was attached to beam 1 using a stinger. The exciter was located 0.36 m from the right-hand end of beam 1. A scanning laser vibrometer was used for the vibration response measurements.

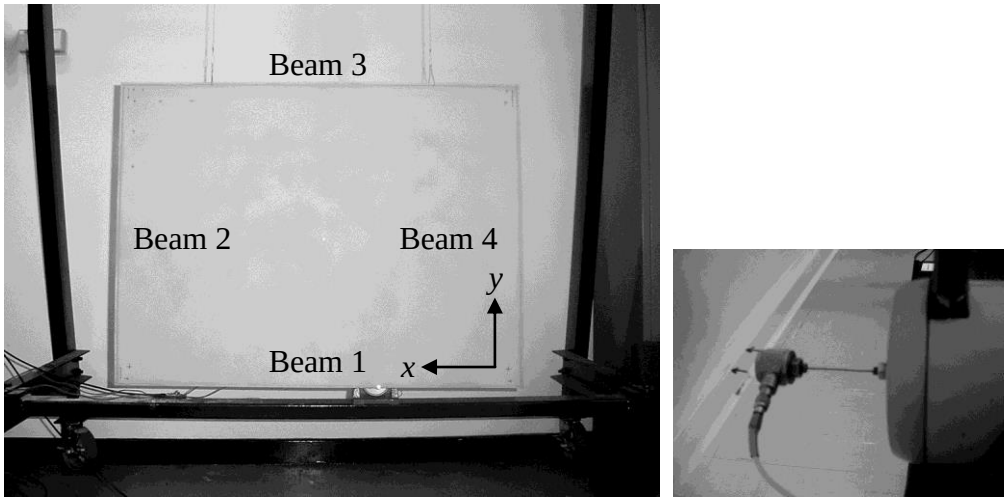


Figure 10. Experimental configurations for the measurement of mobilities and the attachment of the exciter.

## 7.2 Energy and powers in the fully framed structure consisting of similar beams

This section deals with coupled structure F1, a system consisting of a rectangular plate surrounded by four similar beams. The experimental results are compared here with the calculated responses using both the modal and wave methods. The spatially averaged energy is estimated from the transfer mobilities obtained at randomly selected measurement points (10 points for each beam and 20 points for the plate).

The calculated and measured input power are compared in Figure 11 in terms of one-third octave band spectra. The results of the modal and the wave models show a close agreement with each other except at low frequencies. Moreover, the numerical and

experimental results are in good agreement, at least between 40 and 300 Hz. At high frequencies, the added mass (14 g) of the force transducer affects the experimental results [2,22]. The mass effect has been allowed for in the case of the wave method by adding it to the prediction; then the difference between the numerical model and the experiment in one-third octave bands is 1.2 dB on average above 40 Hz. In the remaining, results in terms of energy ratios eliminate this added mass effect.

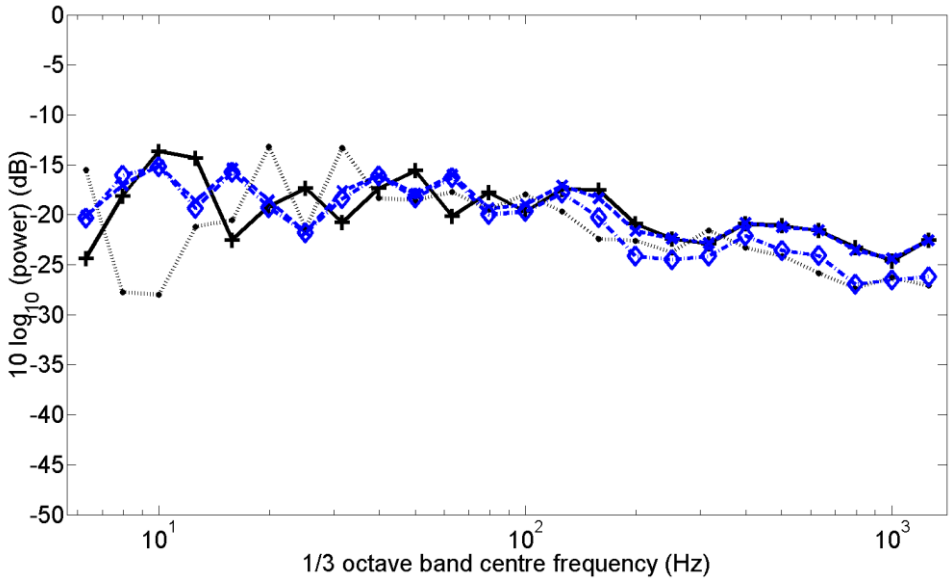


Figure 11. Input power in one-third octave bands for the four-beam-plate system F1: comparison between the numerical models and the experiment. - -+- , modal method; −×−, wave method; ·−◇·−, wave method with mass effect; ···•···, experiment.

Figure 12 shows the energy ratios of beams 2, 3 and 4 to the driven beam (beam 1) from the experimental results (the energy ratio of the plate will be shown in Figure 13). In the absence of the plate, as beam 3 receives only small amount of energy from beams 2 and 4, it can be expected that beam 3, the farthest beam from the excitation point, will possess the lowest energy level compared with beams 2 and 4; however, in fact, the energy level of beam 3 is higher than the other two beams, which means that more energy is transferred to beam 3 through the plate than through the other beams.

Note that the driven beam and beam 3 are identical. Thompson et al. [3] showed that energy transfer to an opposite beam is maximized when the two beams are identical for a beam-plate-beam structure. It seems that such a phenomenon also occurs for the beam-framed structure. If the two parallel beams in this framed structure are not identical, this phenomenon is no longer observed, as will be discussed in Section 7.3.

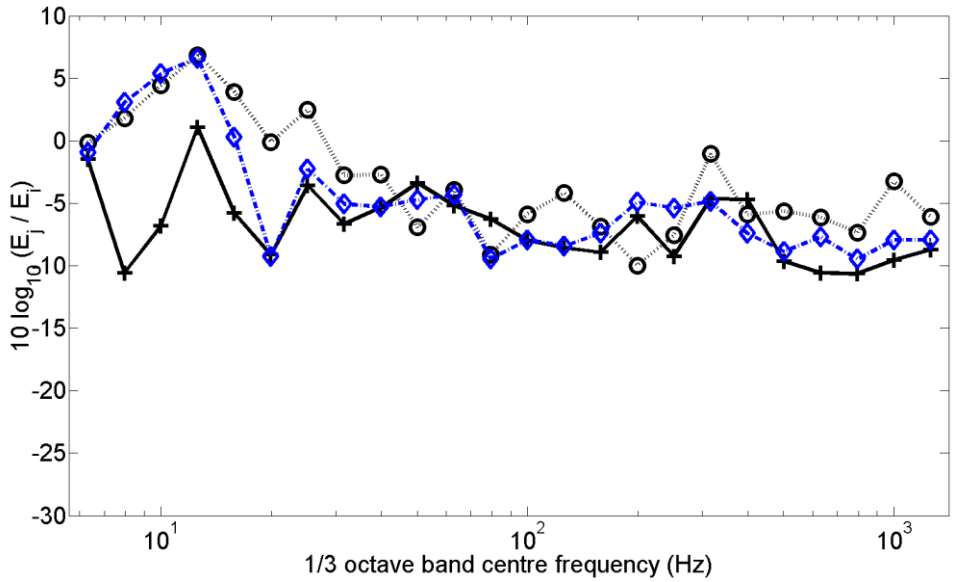


Figure 12. Energy ratio in one-third octave bands of four-beam-plate system F1 (experiment): --+-- , $E_{beam2}/E_{beam1}$ ; ··· O ···, $E_{beam3}/E_{beam1}$ ; ·–◇·– , $E_{beam4}/E_{beam1}$ .

Figure 13 compares the energy ratios in one-third octave bands from the experiments and the theoretical models. In the wave method, the approximate plate energy of the framed structure is found from the sum of the energies of the separate plates connected to each beam. For the energy ratio of the plate relative to beam 1, above about 40 Hz both the predicted and experimental results agree very well, within about 3 dB. Similar to Section 6.3, the energy ratio of the plate is mostly higher than the beam's energy ratio (see the dissipated powers in Figure 9). For other cases, except for beam 3, the maximum difference between the wave method and the experiment is less than about 5 dB in the mid and high frequency regions, even though the wave method is known to provide an approximate response. Beam 3 has a similar energy ratio in the experiments and the modal method, whereas in the wave method it was up to 10 dB lower. The large difference for beam 3 is due to the modelling assumption in the wave method. Moreover, the numerical results for beams 2 and 4 are quite similar. This implies that the energy transfer mechanism of these beams is different from beam 3, as explained earlier. Beam 4, which was closer to the excitation point with the same cross section, possesses a very similar energy level in the two numerical models.

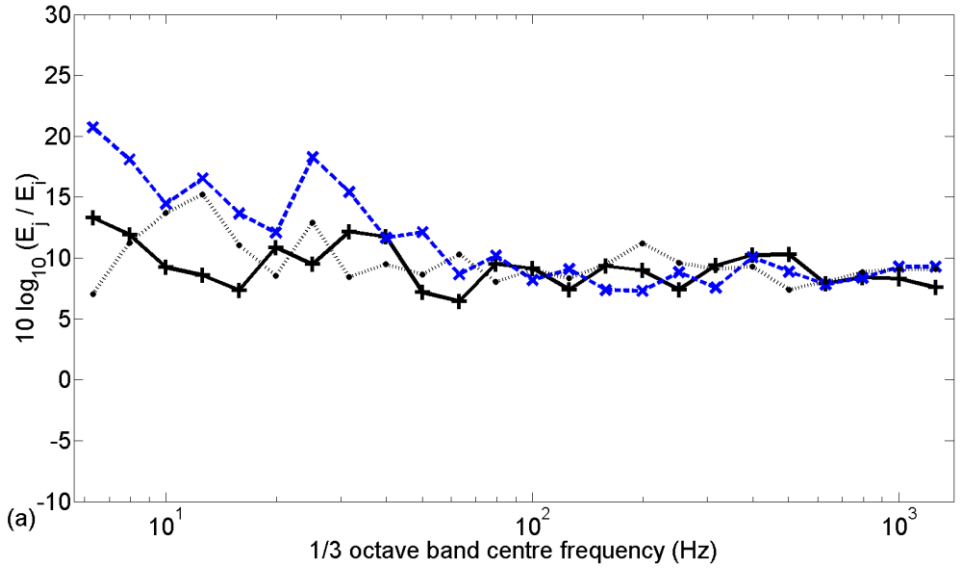
30
25
20
15
10
5
0
-5
-10
10 log10(Ej / Ei)
(a)
10^1
10^2
10^3
1/3 octave band centre frequency (Hz)

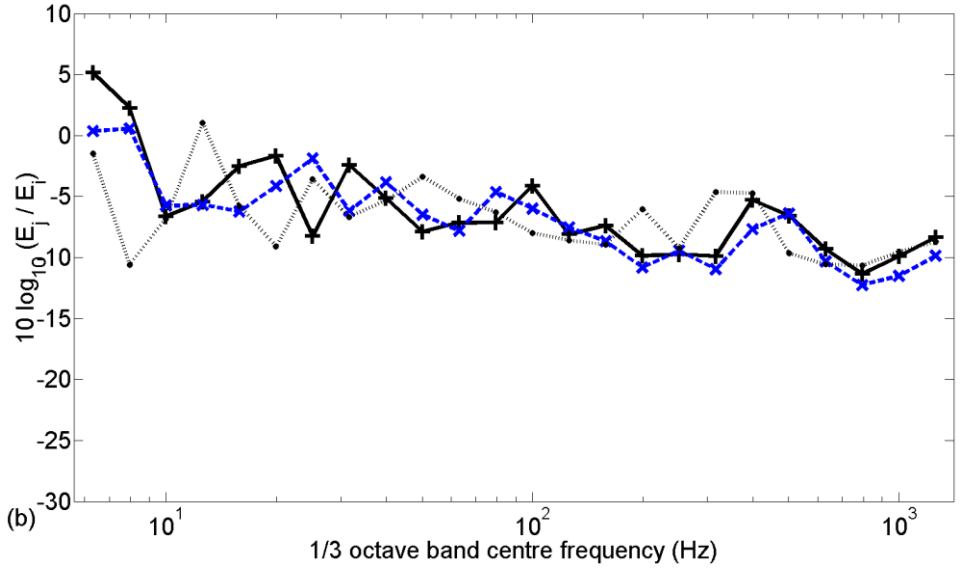
10
5
0
-5
-10
-15
-20
-25
-30
10 log10(Ej / Ei)
(b)
10^1
10^2
10^3
1/3 octave band centre frequency (Hz)

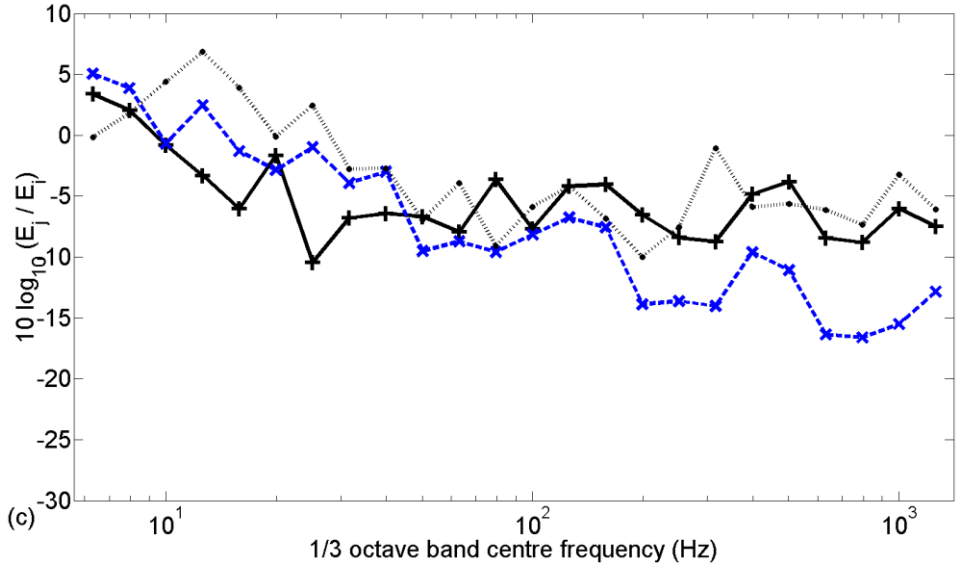
10
5
0
-5
-10
-15
-20
-25
-30
10 log10(Ej / Ei)
(c)
10^1
10^2
10^3
1/3 octave band centre frequency (Hz)

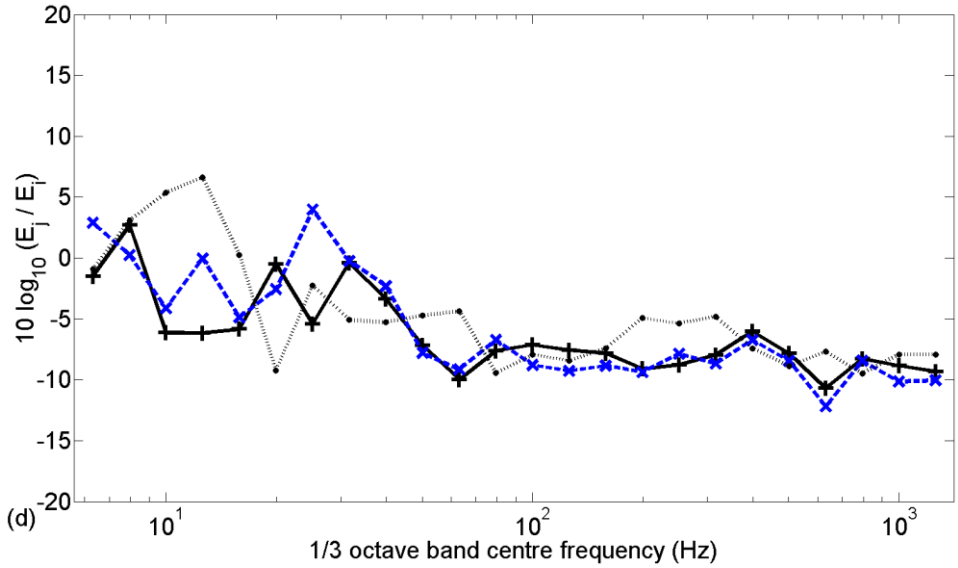


Figure 13. Energy ratio in one-third octave bands of four-beam-plate system F1: (a) $E_{plate}/E_{beam1}$, (b) $E_{beam2}/E_{beam1}$, (c) $E_{beam3}/E_{beam1}$, (d) $E_{beam4}/E_{beam1}$. - - + -, modal method; $-\times-$, wave method; $\cdots\bullet\cdots$, experiment.

### 7.3 Energy and power in the fully framed structure consisting of dissimilar beams

The same investigation has been carried out for the coupled system F2. Adjacent beams 1 and 4 are 24.1 mm high, and beams 2 and 3 are 13.3 mm high.

The ratios of the energies of beams 2, 3 and 4 to the driven beam obtained from the experiment are shown in Figure 14. It can be seen that the energy level of beam 4, which is closer to the excited beam and the excitation point, is always higher than those of the other beams above 150 Hz. This is not because the energy ratio of beam 4 is increased (note that the energy ratios of beam 4 are similar in Figures 12 and 14) but because the energy ratio of beam 3 is decreased. This occurs because beam 3 is not identical to the driven beam (recall that the energy of beam 3 is maximized when identical to the driven beam).

Furthermore, the energy ratio of beam 2 is always lower than those of the other beams. It can be observed that this energy ratio is clearly lower when compared to that presented in Figure 12. This means that the energy attenuation from beam 1 to beam 2 is increased, because the beam sections are different.

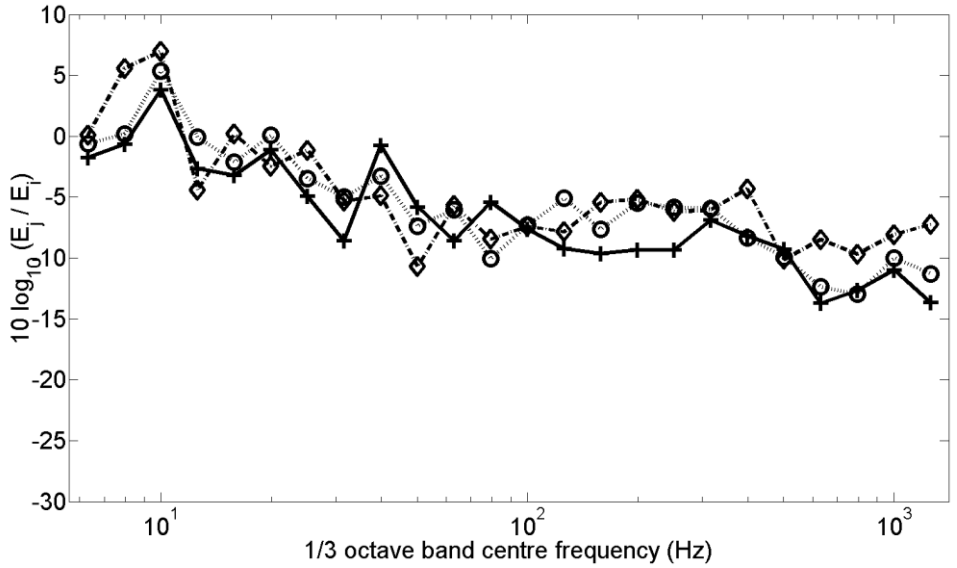


Figure 14. Energy ratio in one-third octave bands of four-beam-plate system F2 (experiment): --+-- , $E_{beam2}/E_{beam1}$ ; ··· O ···, $E_{beam3}/E_{beam1}$ ; ·–◇·– , $E_{beam4}/E_{beam1}$ .

The energy ratios found numerically and experimentally are compared in Figure 15. First, when comparing Figures 15 and 13, the energy ratios of the plate and beam 4 above 80 Hz are almost the same between systems F1 and F2. This means that the changes of beams 2 and 3 do not have a significant impact on the behaviours of the plate and beam 4.

The modal model has a close agreement with the experimental results for all cases. The wave model shows reasonable agreement with experiment above about 40 Hz for the energy ratios of the stiffer beams and the plate; however, it was found that the agreement for beam 3 reduces compared with the case in which all of the beams were identical, and there was also a difference for beam 2. In both cases, the wave model gives lower energy ratios than for the identical beams, whereas the modal method gives similar results. This appears to be fundamentally due to the fact that the wave model does not physically connect these beams to the excited beam through the plate. Furthermore, as pointed out by Thompson et al., if a non-driven beam is less stiff, then the motion of the non-driven beam is dominated by the waves with the wavenumber of the stiff-driven beam [3]; however, the wavenumber of the non-driven beam in this wave model differs from that of the driven beam, which may result in a discrepancy between the response of the wave model and the experimental result.

The difference between the energy ratios found from the wave method and the experiment in Figure 15 (b) (beam 2) increases compared to that observed in Figure 13 (b). The cross section of beam 2 is different from beam 1, which results in a large energy reflection at the junction. Also, beam 2 is located far from the excitation point. This means that the influence of the plate on beam 2 is greater; however, the physical connection between the beams through the plate is missing in the wave model, and the difference between the wave model and the real situation is highlighted. On the other

hand, as beam 4 receives higher energy directly from the excited beam, the influence of the plate is relatively small.

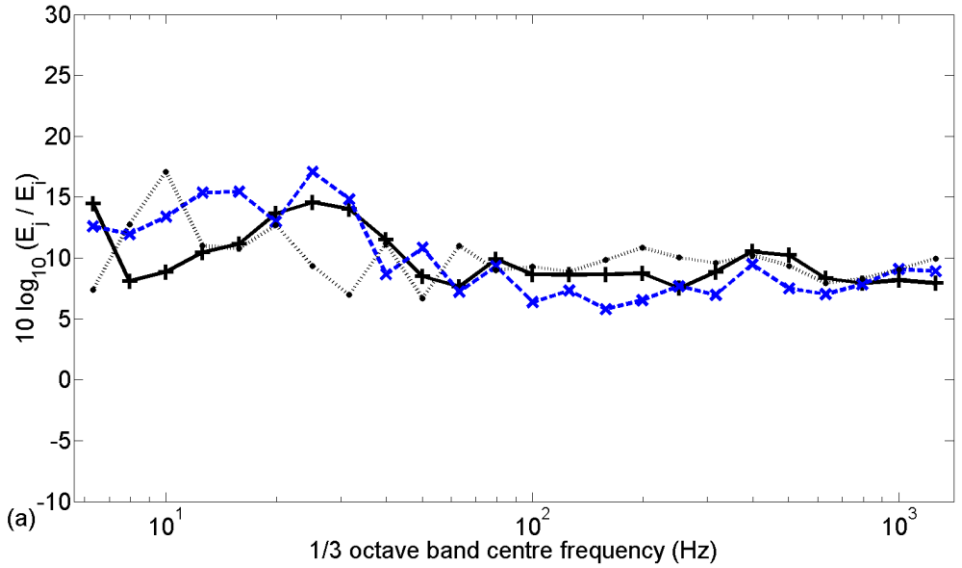
30
25
20
15
10
5
0
-5
-10
10 log10(Ej / Ei)
(a)
10^1
10^2
10^3
1/3 octave band centre frequency (Hz)

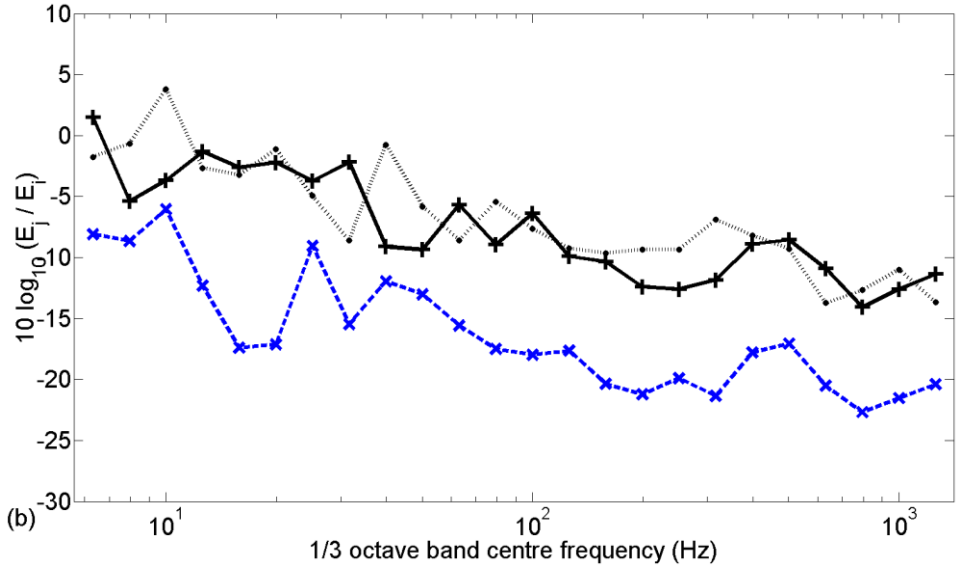
10
5
0
-5
-10
-15
-20
-25
-30
10 log10(Ej / Ei)
(b)
10^1
10^2
10^3
1/3 octave band centre frequency (Hz)

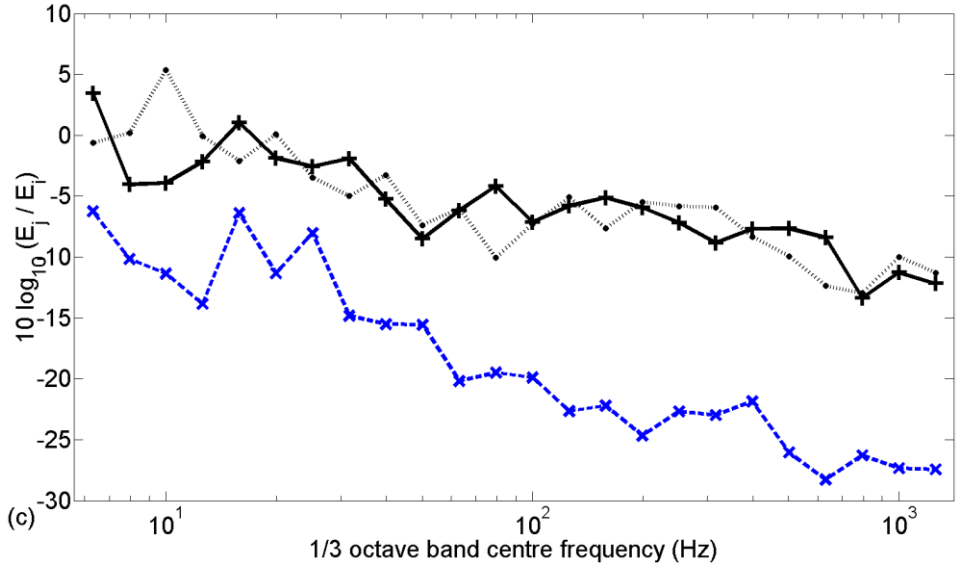
10
5
0
-5
-10
-15
-20
-25
-30
10 log10(Ej / Ei)
(c)
10^1
10^2
10^3
1/3 octave band centre frequency (Hz)

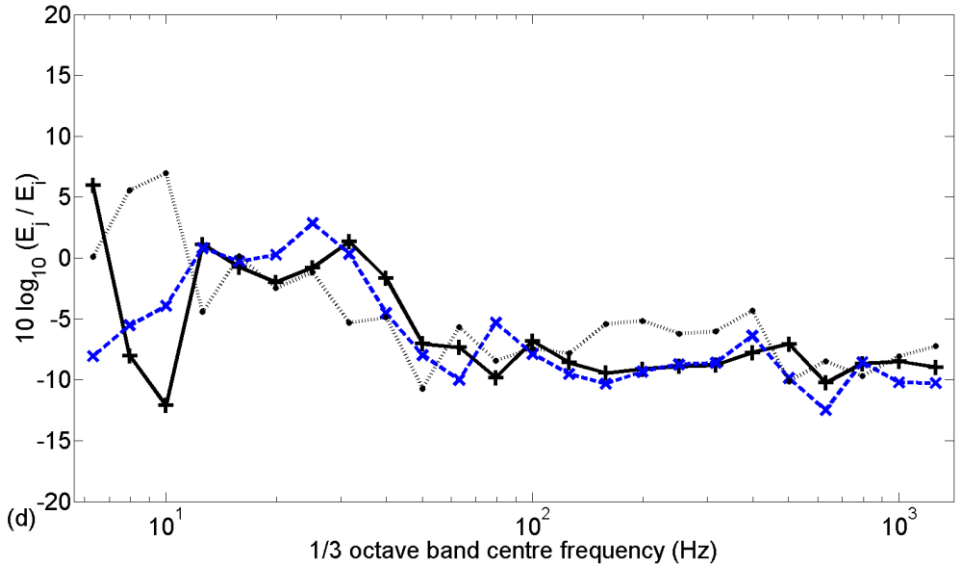


Figure 15. Energy ratio in one-third octave bands of the four-beam-plate system F2: (a) $E_{plate}/E_{beam1}$, (b) $E_{beam2}/E_{beam1}$, (c) $E_{beam3}/E_{beam1}$, (d) $E_{beam4}/E_{beam1}$. - -+- , modal method; −×−, wave method; ⋯•⋯, experiment.

## 8. Discussion

The motion of a coupled system consisting of four beams surrounding a rectangular plate can be obtained relatively simply using the modal method by assuming sliding boundary conditions at the edges of the rectangular plate. Such an assumption of the sliding boundary condition may be applicable for this particular framed structure surrounded by beams with large cross section. Although the sliding condition is not a necessary condition in the modal method, it reduces the complexity in its application due to the use of the separation of the variables for the plate and the fact that the plate and beam mode shapes are identical. Strictly, although such boundary conditions are different from the experiment, the differences introduced are not very significant, at least regarding the mid- and high frequency regions and considering the frequency band average results.

The wave method predicts only an approximate response. By assuming most of the power input from an excitation is dissipated in the plate, the framed system can be modelled as a system consisting of four beams, each attached to a separate plate. The dimensions and the boundary conditions of the four plates were assumed to be the same as the original plate surrounded by four beams. Thus, the opposite edge parallel to the beam was assumed to be sliding. The response in terms of one-third octave band averages showed that this plate-decoupled wave model provides reasonable results, primarily for power input and power dissipation, compared with the modal model, at least above 50 Hz.

## 9. Conclusions

In this study, the aim was to understand the response of a framed structure consisting of stiff beams and a flexible plate using both modal and wave models and to compare the

power and energy levels between the components, concentrating mainly on the so-called mid-frequency region.

Although the sliding boundary conditions of the analytical models differed from those in the experiment, the input power comparison in terms of one-third octave band averages showed the suitability of the numerical models at mid and high frequencies. The investigation on the power relationship shows that most of the energy is dissipated by the flexible plate in this framed structure.

The energy ratio between components based on one-third octave bands also shows the applicability of the numerical models, as the results are generally in close agreement with the experiments. The modal model appears to be appropriate to describe the energy relationship between the beams and plate. The wave model shows some limitations in predicting the energy of beams remote from the excitation; however, it can reasonably estimate the energy level of the driven beam and the plate.

The comparison of the modal and wave models clearly shows that the energy is transmitted from the driven beam to the opposite beam through the plate in the framed structure. The difference between the two numerical models increases in estimating the energy level of the opposite beam when it has an identical cross-section to the driven beam. This is because the wave model cannot describe the physical connection via the plate between the two parallel beams, which plays a crucial role in transferring the energy in this particular case.

It has previously been shown [3] that the energy transfer between two parallel beams in a beam-plate-beam structure is maximized when the two beams are identical. The present study shows that such a phenomenon also holds for a framed structure.

## Funding

This research received no specific grant from any funding agency in the public, commercial, or not-for-profit sectors.

## References

1. Grice RM and Pinnington RJ. A method for the vibrational analysis of built-up structures, part 1: Introduction and analytical analysis of the plate-stiffened beam. *J Sound Vib* 1999; 230: 825-849.
2. Yoo JW. Investigations of power flow mechanism and passive energy control using an energy-absorbing plate in beam-plate structures. *J Syst Des Dyn* 2007; 1: 1-12.
3. Thompson DJ, Ferguson NS, Yoo JW and Rohlfing J. Structural waveguide behaviour of a beam-plate system. *J Sound Vib* 2008; 318: 206-226.
4. Rumerman ML. Vibration and wave propagation in ribbed plates. *J Acoust Soc Am* 1975; 57: 370–373.
5. Legault J and Atalla N. Sound transmission through a double panel structure periodically coupled with vibration insulators. *J Sound Vib* 2010; 329: 3082-3100.

6. Hammer P and Petersson B. Strip excitation, part I: Strip mobility. *J Sound Vib* 1989; 129: 119-132.
7. Dickow KA, Brunskog J and Ohlrich M. Modal density and modal distribution of bending wave vibration fields in ribbed plates. *J Acoust Soc Am* 2013; 134: 2719–2729.
8. Ji L, Mace BR and Pinnington RJ. A hybrid mode/Fourier-transform approach for estimating the vibrations of beam-stiffened plate systems. *J Sound Vib* 2004; 274: 547-565.
9. Seo S-H and Hong S-Y and Kil H-G. Power flow analysis of reinforced beam-plate coupled structures. *J Sound Vib* 2003; 259: 1109-1129.
10. Yoo JW. *Dynamic modelling of beam-plate systems in the mid-frequency region.* PhD Thesis, University of Southampton, UK, 2005.
11. Takabatake H and Nagareda Y. A simplified analysis of elastic plates with edge beams. Comput Struct 1999; 70: 129-139.
12. Yang J and Gupta A. Ritz vector approach for static and dynamic analysis of plates with edge beams. *J Sound Vib* 2002; 253: 373-388.
13. Grice RM and Pinnington RJ. Analysis of the flexural vibration of a thin-plate box using a combination of finite element analysis and analytical impedance. *J Sound Vib* 2002; 249: 499-527.
14. Langley RS, Shorter PJ and Cotoni V. A hybrid FE-SEA method for the analysis of complex vibro-acoustic systems. *Proc NOVEM* , St. Raphael, France, 2005.
15. Castanier MP and Pierre C. Mid-frequency vibration analysis of complex structures: State of the art and future directions. In: 10th Inter Congress Sound Vibration, Stockholm, 2003; pp.1123-1130.
16. Warburton GB. *The Dynamical Behaviour of Structures.* 2nd ed. Oxford: Pergamon Press, 1976.
17. Ji L, Mace BR and Pinnington RJ. A mode-based approach for the mid-frequency vibration analysis of coupled long- and short-wavelength structures. *J Sound Vib* 2006; 289: 148-170.
18. Langley RS. Application of the dynamic stiffness method to the free and forced vibrations of aircraft panels. *J Sound Vib* 1989; 135: 319-331.
19. Meirovich L. *Elements of Vibration Analysis*. 2nd ed. New York: McGraw-Hill, 1986.
20. Yoo JW. Modelling of sound radiation from a beam-stiffened plate and a clamped rectangular plate based on a modal method. *J Mech Eng Sci* 2014; 228: 2900–2914.
21. Strasberg M and Feit D. Vibration damping of large structures induced by attached small resonant structures. *J Acoust Soc Am* 1996; 99: 335-344.
22. Cremer L, Heckl M and Ungar EE. *Structure-borne Sound*. 2nd ed. Berlin: Springer Verlag, 1988.